

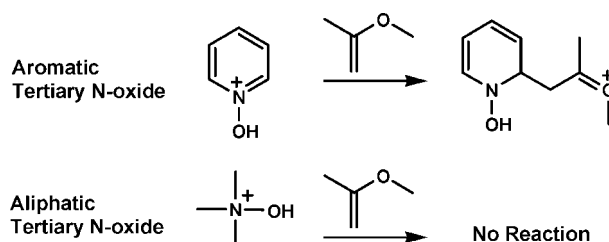
Identification of the Aromatic Tertiary N-Oxide Functionality in Protonated Analytes via Ion/Molecule Reactions in Mass Spectrometers

Penggao Duan,[†] Todd A. Gillespie,[‡] Brian E. Winger, and Hilkka I. Kenttämaa^{*,†}

Department of Chemistry, Purdue University, West Lafayette, Indiana 47907, and Eli Lilly and Company, Indianapolis, Indiana 46285

hilkka@purdue.edu

Received February 6, 2008



A mass spectrometric method is presented for the rapid identification of compounds that contain the aromatic *N*-oxide functional group. This method utilizes a gas-phase ion/molecule reaction with 2-methoxypropene that yields a stable adduct for protonated aromatic tertiary *N*-oxides (and with one protonated nitron) in different mass spectrometers. A variety of protonated analytes with O- or N-containing functional groups were examined to probe the selectivity of the reaction. Besides protonated aromatic tertiary *N*-oxides and one nitron, only three protonated amines were found to form a stable adduct but very slowly. All the other protonated analytes, including aliphatic tertiary *N*-oxides, primary *N*-oxides, and secondary *N*-oxides, are unreactive toward or react predominantly by proton transfer with 2-methoxypropene.

Introduction

The oxidation of a N-atom to form an *N*-oxide is an important biotransformation pathway for many drugs and a commonly observed stress-induced oxidative degradation reaction in pharmaceuticals.¹ The ability to rapidly identify metabolites and degradation products containing the *N*-oxide functionality is of interest since they are usually considered to be genotoxic.^{2,3} Spectroscopic techniques, such as FT-IR and X-ray crystallography, are commonly used to obtain information regarding the elemental connectivity of analytes. However, both techniques require time-consuming isolation of the components of prior to analysis and relatively large quantities of high-purity samples. NMR typically provides detailed structural information for analytes but is hindered by the requirement of high-purity

samples with good solubility.⁴ Furthermore, the low natural abundance of ¹⁵N (0.37%) relative to ¹⁴N makes it difficult to detect N-containing species. Finally, the very small differences in chemical shifts of many N-containing compounds complicate NMR spectral interpretation.⁵ Tandem mass spectrometric methods involving collision-activated dissociation (CAD) have been widely used for structure elucidation of unknown compounds directly in mixtures. However, the CAD spectra of *N*-oxides are, in general, quite similar to those of many other N-containing species, which makes it difficult to unambiguously identify the *N*-oxide functionality.^{4,6} For example, the CAD mass spectrum of protonated 4-amino-3,5-dichloropyridine *N*-oxide is identical with that of its isomer, protonated 4-amino-3,4-dichloro-2-hydroxypyridine.⁶

Recently, a mass spectrometry method based on atmospheric pressure chemical ionization (APCI) or electrospray ionization

* Corresponding author. Phone: 765 494-0882. Fax: 765 494-0239.

[†] Purdue University.

[‡] Eli Lilly and Company.

(1) Clement, B. *Biomed. Health Res.* **1998**, *25*, 59–71.

(2) Ashby, J.; Tennant, R. W. *Mutat. Res.* **1988**, *204*, 17–115.

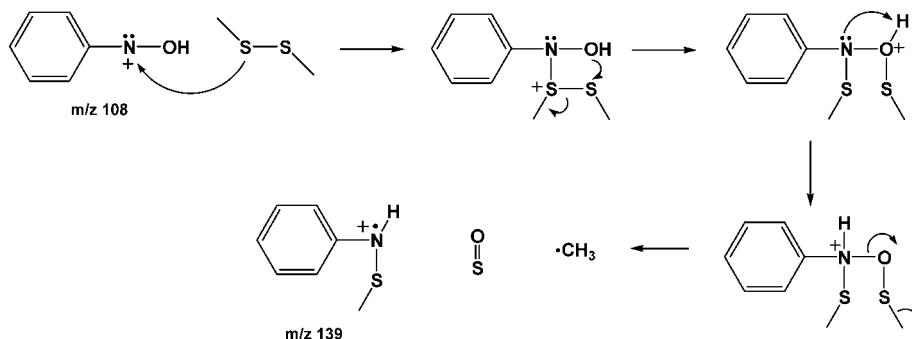
(3) Ashby, J.; Tennant, R. W.; Zeiger, E.; Stasiewicz, S. *Mutat. Res.* **1989**, *223*, 73–103.

(4) Peiris, D. M.; Lam, W.; Michael, S.; Ramanathan, R. *J. Mass Spectrom.* **2004**, *39*, 600–606.

(5) Nelson, J. H. *Nuclear Magnetic Resonance Spectroscopy*; Pearson Education: Upper Saddle River, NJ, 2003.

(6) Tong, W.; Chowdhury, S. K.; Chen, J.-C.; Zhong, R.; Alton, K. B.; Patrick, J. E. *Rapid Commun. Mass Spectrom.* **2001**, *15*, 2085–2090.

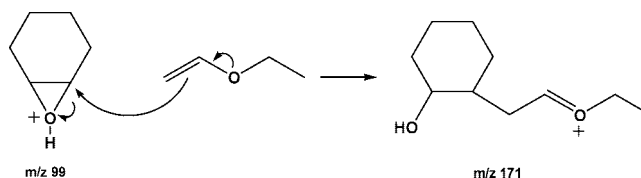
SCHEME 1



(ESI) was introduced to distinguish two types of isomeric N-containing compounds that are commonly formed during drug metabolism: *N*-oxides (formed upon N-oxidation) and N-containing alcohols (formed upon hydroxylation of C-atoms in N-containing compounds). This method is based on diagnostic deoxygenation of *N*-oxides during thermal degradation in a heated APCI or ESI source, which does not occur for their hydroxy isomers.^{4,6,7} However, thermal degradation can be so severe that the intact protonated *N*-oxide is not observed at all. For example, up to 74% of cocaine *N*-oxide is converted into cocaine and norcocaine during LC/APCI-MS analysis.⁸ Further, quantitative analysis based on thermal degradation methods can be problematic.⁴

Tandem mass spectrometric methods based on ion/molecule reactions (instead of dissociation) hold great promise for being able to provide information useful in the identification of specific functional groups in analytes.⁹ In most cases, selective ionic reagents have been used to probe specific functionalities in neutral analytes. For example, the epoxide and the acetal functionalities can be identified on the basis of reactions with acylium ions,^{10a,b} and the enol ether functionality on the basis of reactions with cationic 2-azabutadienes via a polar [4⁺ + 2] cycloaddition.^{10c} However, despite the wide use of ionization techniques, such as atmospheric pressure chemical ionization (APCI) and electrospray ionization (ESI), to produce protonated gaseous analytes, only very few studies have focused on the use of a neutral reagent to identify the functionalities in protonated analytes. These studies include the demonstration that ethyl vinyl ether can be used to identify the protonated β -hydroxycarbonyl functionality,^{11a} (*N,N*-diethylamino)dimethylborane can be used to identify the protonated amido functionality,^{11b} and trimethoxyborane and diethylmethoxyborane can be used to identify different types of protonated

SCHEME 2



oxygen-containing functionalities.^{11c,d} We recently reported a method for the identification of the primary *N*-oxide functionality via a functional group selective ion/molecule reaction of the protonated analyte with dimethyl disulfide (DMDS).¹² The mechanism proposed for this reaction (Scheme 1) is not feasible for tertiary *N*-oxides. Indeed, protonated pyridine *N*-oxide was found to be unreactive toward DMDS. Therefore, a different reagent is needed for the identification of the tertiary *N*-oxide functional group.

In this followup study, we introduce 2-methoxypropene (MOP) as a reagent that can be used to identify the aromatic tertiary *N*-oxide functionality in protonated analytes. 2-Methoxypropene forms a stable adduct selectively with protonated aromatic tertiary *N*-oxides (and also with one protonated nitrone) in Fourier transform ion cyclotron resonance (FT-ICR) and triple quadrupole (TSQ) mass spectrometers.

Results and Discussion

In the search for a suitable reagent, ethyl vinyl ether appeared as a promising candidate since it is known to react with protonated cyclohexene oxide to form an adduct in the gas phase (Scheme 2).¹³ This type of a reaction may also occur for protonated analytes with a tertiary *N*-oxide functional group since the partially positively charged α -carbon atom of a protonated tertiary *N*-oxide should be susceptible to nucleophilic attack. Therefore, the reaction of protonated pyridine *N*-oxide with ethyl vinyl ether was examined. As expected, ethyl vinyl ether indeed forms a stable addition product with protonated pyridine *N*-oxide. However, this reaction is extremely slow. A similar but more nucleophilic reagent is therefore needed to promote faster addition.

To identify such a reagent, the reactions of protonated pyridine *N*-oxide were examined with several additional nucleophilic alkenes, including cyclopentene, cyclohexene, and 1,3- and 1,4-cyclohexadienes. No reactions were observed. Therefore, a more nucleophilic reagent, 2-methoxypropene

(7) Ramanathan, R.; Su, A. D.; Alvarez, N.; Blumenkrantz, N.; Chowdhury, S. K.; Alton, K.; Patrick, J. *Anal. Chem.* **2000**, *72*, 1352–1359.

(8) Lin, S.-N.; Walsh, S. L.; Moody, D. E.; Foltz, R. L. *Anal. Chem.* **2003**, *75*, 4335–4340.

(9) For examples, see: (a) Eichmann, E. S.; Brodbelt, J. S. *Org. Mass Spectrom.* **1993**, *28*, 1608–1615. (b) Alvarez, E. J.; Brodbelt, J. S. *J. Mass Spectrom.* **1995**, *30*, 625–631. (c) Ramos, L. E.; Cardoso, A. M.; Correia, A. J. F.; Nibbering, N. M. M. *Int. J. Mass Spectrom.* **2000**, *203*, 101–110. (d) Moraes, L. A. B.; Gozzo, F. C.; Eberlin, M. N.; Vainiotalo, P. J. *Org. Chem.* **1997**, *62*, 5096–5103. (e) Eberlin, M. N. *J. Mass Spectrom.* **2006**, *41*, 141–156. (f) Brodbelt, J. S. *Mass Spectrom. Rev.* **1997**, *16*, 91–110.

(10) (a) Moraes, L. A. B.; Eberlin, M. N. *Chem.-Eur. J.* **2000**, *6*, 897–905. (b) Eberlin, M. N.; Cooks, R. G. *Org. Mass Spectrom.* **1993**, *28*, 679–687. (c) Meurer, E. C.; Eberlin, M. N. *Int. J. Mass Spectrom.* **2001**, *210*, 469–482.

(11) (a) Kenttämä, H. I.; Cooks, R. G. *J. Am. Chem. Soc.* **1989**, *111*, 4122–4123. (b) Campbell, K. M.; Watkins, M. A.; Li, S.; Fiddler, M. N.; Winger, B.; Kenttämä, H. I. *J. Org. Chem.* **2007**, *72*, 3159–3165. (c) Watkins, M. A.; Price, J. M.; Winger, B. E.; Kenttämä, H. I. *Anal. Chem.* **2004**, *76*, 964–976. (d) Somuramasami, J.; Duan, P.; Watkins, M. A.; Winger, B. E.; Kenttämä, H. I. *Int. J. Mass Spectrom.* **2007**, *265*, 359–371.

(12) Watkins, M. A.; WeWora, D. V.; Li, S.; Winger, B. E.; Kenttämä, H. I. *Anal. Chem.* **2005**, *77*, 5311–5316.

(13) Kenttämä, H. I.; Pachuta, R. R.; Rothwell, A. P.; Cooks, R. G. *J. Am. Chem. Soc.* **1989**, *111*, 1654–1665.

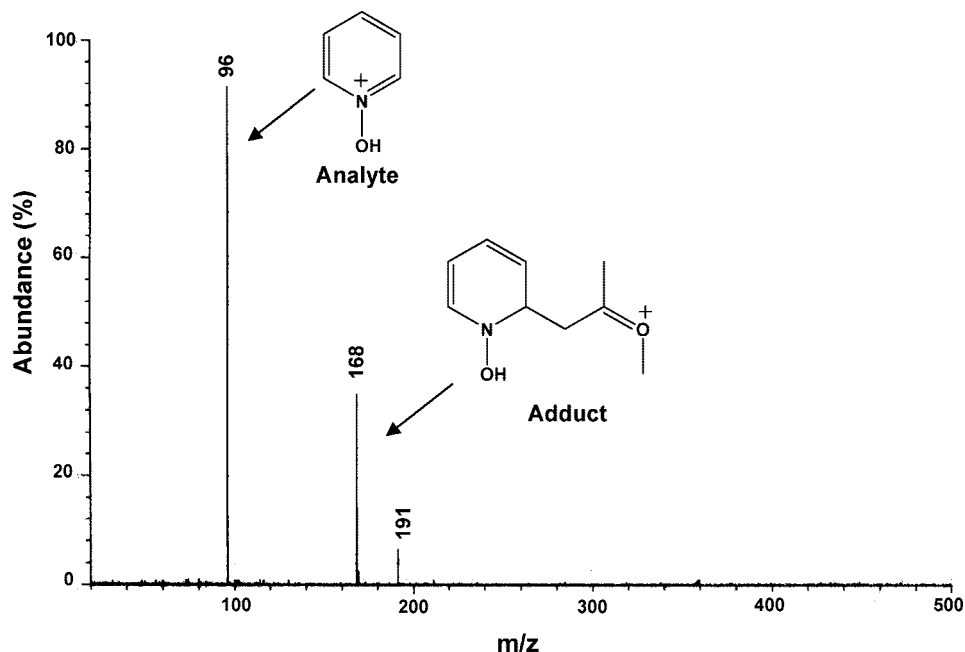
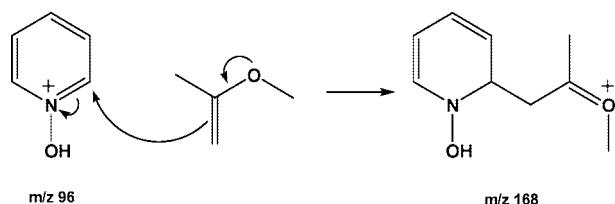


FIGURE 1. Product ion mass spectrum measured after 9 s reaction of protonated pyridine *N*-oxide with 2-methoxypropene present at a nominal pressure of 5.9×10^{-8} Torr in an FT-ICR. Abundant addition product of *m/z* 168 is evident. The ion of *m/z* 191 is a proton-bound dimer of pyridine *N*-oxide.

SCHEME 3



(MOP), was tested (based on their proton affinities (PAs), MOP should be more nucleophilic than ethyl vinyl ether: the PAs are 214 kcal/mol¹⁴ and 208 kcal/mol,¹⁴ respectively). Indeed, MOP was found to react with protonated pyridine *N*-oxide about ten times faster than with ethyl vinyl ether, leading to the formation of a stable adduct (Figure 1). The mechanism probably involves a nucleophilic attack by the π -electrons of the C–C double bond of MOP at the partially positively charged α -carbon atom of the protonated *N*-oxide (Scheme 3). This mechanism is supported by the observation that CAD leads to exclusive loss of the MOP molecule to reproduce the protonated pyridine *N*-oxide.

Examination of a series of tertiary *N*-oxides revealed that protonated *aromatic* tertiary *N*-oxides form an adduct with MOP while protonated *aliphatic* tertiary *N*-oxides are unreactive (Table 1). A protonated nitron, 5,5-dimethyl-1-pyrroline *N*-oxide, was also found to react with MOP by addition. These findings suggest that a C=N double bond at the *N*-oxide functionality is necessary for the adduct formation, and hence support the proposed mechanism (Scheme 3). Another protonated nitron, *N*-benzylidene-*tert*-butylamine *N*-oxide, was found to be unreactive toward MOP, possibly due to steric hindrance.

The selectivity of MOP for the protonated *aromatic* tertiary *N*-oxide functionality was probed by examining its reactivity

toward various protonated analytes containing O- or N-functional groups (Tables 2 and 3). The only reaction observed for protonated analytes with PA lower than that of MOP was proton transfer to MOP, with two exceptions. Besides proton transfer product, 2-nitrosotoluene (a primary *N*-oxide) and 2,2,6,6-tetramethylpiperidine *N*-oxide (TEMPO, a secondary *N*-oxide) also form a stable adduct but in very low abundance (Table 3). All protonated analytes with PA higher than that of MOP are unreactive toward MOP (Table 3), with the exception of three protonated *N*-containing analytes, 1-hexanamine, 3-hydroxypyridine, and pyridine, that form an adduct with MOP albeit extremely slowly (~ 10 to 40 times slower than protonated aromatic tertiary *N*-oxides).

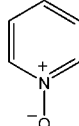
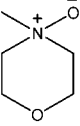
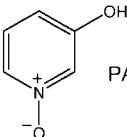
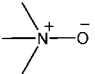
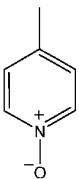
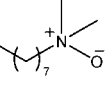
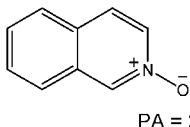
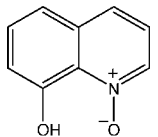
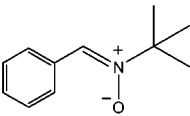
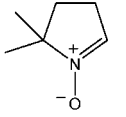
The above results demonstrate that MOP can be used to distinguish *aromatic* tertiary *N*-oxides from *aliphatic* tertiary *N*-oxides as well as from primary and secondary *N*-oxides. Protonated *aromatic* tertiary *N*-oxides react by addition to MOP, protonated *aliphatic* tertiary *N*-oxides are unreactive toward MOP, and protonated primary and secondary *N*-oxides react with MOP predominantly by proton transfer. It is worth pointing out that protonated primary and secondary *N*-oxides can be differentiated based on the fact that dimethyl disulfide selectively reacts with protonated primary *N*-oxides and is unreactive toward secondary *N*-oxides in the gas phase.¹²

The selective adduct formation for only protonated tertiary aromatic *N*-oxides shows no dependence on the PA of the *N*-oxide, as expected based on the proposed mechanism. Since only one product, the adduct, is formed in the reaction of MOP with protonated aromatic tertiary *N*-oxides, the mass spectra are easy to interpret. Due to the high basicity of *N*-oxides, their protonated forms are unreactive toward most small neutral reagents, which facilitates their identification.

In an effort to demonstrate the applicability of this method to mass spectrometers other than FT-ICR, it was adapted to a Finnigan TSQ 700 triple quadrupole mass spectrometer. The analyte, pyridine *N*-oxide, was protonated in a CI source, mass selected with the first quadrupole, and allowed to undergo

(14) Hunter, E. P.; Lias, S. G. Proton Affinity Evaluation. In *NIST Chemistry WebBook, NIST Standard Reference Database*; Linstrom, P. J., Mallard, W. G., Eds.; National Institute of Standards and Technology: Gaithersburg, MD, June 2005; No. 69 (<http://webbook.nist.gov>).

TABLE 1. Tertiary N-Oxides, Their PAs (in kcal/mol), Reactions of Their Protonated Forms with 2-Methoxypropene (PA = 214 kcal/mol^c) and the Reaction Efficiencies^b (Eff.) in the FT-ICR Mass Spectrometer

Tertiary N-oxide (Aromatic)	Observed reaction	Tertiary N-oxide (Aliphatic)	Observed reaction
 PA = 221 ^a	Addition Eff. = 2.5%	 PA = 228 ^d	No reaction
 PA = 222 ^c	Addition Eff. = 1.6%	 PA = 235 ^a	No reaction
 PA = 226 ^c	Addition Eff. = 2.7%	 PA = 228 ^d	No reaction
 PA = 228 ^c	Addition Eff. = 0.6%	Nitrone	Observed reaction
 PA = 228 ^c	Addition Eff. = ~ 2.1% ^e	 PA = 221 ^c	No reaction
		 PA = 221 ^c	Addition Eff. = 1.8%

^a Reference 14. ^b Eff. = reaction efficiency = $k_{\text{reaction}}/k_{\text{collision}} \times 100\%$. ^c Calculated at the B3LYP/6-31G(d) level of theory, using an isodesmic reaction scheme involving pyridine N-oxide as a reference Brønsted acid. ^d Calculated at the B3LYP/6-31G(d) level of theory, using an isodesmic reaction scheme involving trimethylamine N-oxide as a reference Brønsted acid. ^e From nonlinear curve fit: ~40% of the reactant ion population was unreactive.

TABLE 2. O-Containing Analytes, Their PAs^a (in kcal/mol), and Reactions of Their Protonated Forms with 2-Methoxypropene (PA = 214 kcal/mol^c) in the FT-ICR Mass Spectrometer

analyte	proton affinity (PA) (kcal/mol) ^a	obsd reaction
ethanol	186	proton transfer
acetic acid	187	proton transfer
1-propanol	188	proton transfer
acetone	194	proton transfer
diethyl ether	198	proton transfer
benzaldehyde	199	proton transfer
ethyl acetate	200	proton transfer

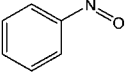
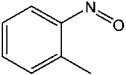
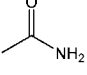
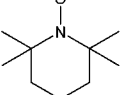
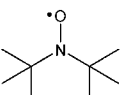
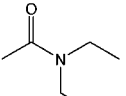
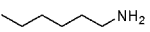
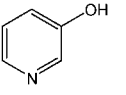
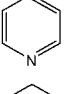
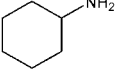
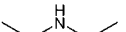
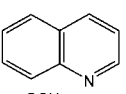
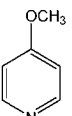
^a Reference 14.

reactive collisions with MOP in the second quadrupole. The ion/molecule reaction products were measured by scanning the third quadrupole. As expected, protonated pyridine N-oxide was found to react with MOP in this mass spectrometer in a similar manner as in FT-ICR (Figure 2). The major product formed is a stable adduct (m/z 168). A small signal for protonated MOP (m/z 73) was also observed due to the higher collision energies in the triple quadrupole (near 0.5 eV or 11.5 kcal/mol) than in FT-ICR.

Conclusions

The ability to use a functional group selective ion/molecule reaction in a mass spectrometer to identify compounds with an aromatic tertiary N-oxide functionality has been demonstrated (one nitrone also undergoes the reaction). Furthermore, this method can be used to distinguish aromatic tertiary N-oxides from primary N-oxides (which can be identified by reaction with dimethyl disulfide¹²) and secondary N-oxides as well as from aliphatic tertiary N-oxides. Almost all protonated analytes examined in this work were found to be unreactive toward or react by proton transfer to MOP. Only protonated aromatic tertiary N-oxides and one nitrone were found to react with MOP to yield an abundant adduct. Protonated primary N-oxide (2-nitrosotoluene) and secondary N-oxide (2,2,6,6-tetramethylpiperidine N-oxide) predominantly undergo proton transfer to MOP, concomitant with the formation of a minor adduct. Although one protonated 1-hexanamine and two pyridines also form adducts with MOP, these reactions are extremely slow. Since one protonated nitrone was found to form an adduct at a rate comparable to those of the aromatic tertiary N-oxides, the possibility of using this method to identify compounds of the

TABLE 3. N-Containing Analytes, Their PAs (in kcal/mol),^a Reactions of Their Protonated Forms with 2-Methoxypropene (PA = 214 kcal/mol^a), and the Reaction Efficiencies^b (Eff.) in the FT-ICR Mass Spectrometer^c

Analyte	Proton affinity ^a (PA) (kcal/mol)	Observed reaction (branching ratio %)
	204	Proton transfer
	Unknown	Proton transfer (96), addition (4) Eff. ^b = 39.8%
	206	Proton transfer
	211	Proton transfer
	Unknown	Proton transfer (93), addition (7) Eff. = ~ 22.4% ^c
	221	No reaction
	222	Addition, Eff. = 0.06%
	222	Addition, Eff. = 0.17%
	222	Addition, Eff. = 0.06%
	223	No reaction
	228	No reaction
	228	No reaction
	230	No reaction

^a Reference 14. ^b Eff. = reaction efficiency = $k_{\text{reaction}}/k_{\text{collision}} \times 100\%$. ^c From nonlinear curve fit: ~18% of the reactant ion population was unreactive.

type $R_2C=N^+-Y$ in general (and not just aromatic *N*-oxides) is currently under investigation.

The excellent agreement between the results obtained by using FT-ICR and a triple quadrupole mass spectrometer suggests that less expensive and more readily available instruments can be adapted to perform this ion/molecule reaction-based screening method. Since this method involves ionization of the analyte by proton transfer, it is applicable to tandem mass spectrometers that are equipped with any common atmospheric pressure ionization (e.g., ESI or APCI) or CI source.

Experimental Section

Chemicals. All compounds studied were commercially available and used without further purification. The purity of all reagents was verified by mass spectrometry.

Instrumentation. The FT-ICR Mass Spectrometer. The Finnigan model FTMS 2001 FT-ICR mass spectrometer used in this work is equipped with a 3-T solenoidal superconducting magnet and an Odyssey data station. The instrument contains a dual cell consisting of two identical cubic 2-in. cells separated by a conductance limit plate. The conductance limit plate has a 2-mm hole in the center for the transfer of ions from one side into the other. The conductance limit plate and the two end trapping plates were maintained at +2.0 V unless otherwise stated. Liquid samples were introduced into the instrument by using either a Varian leak valve or an adjustable leak valve. An automatic solids probe was used to introduce solid samples into the instrument.

The protonated analytes (pressures varied from 1.4×10^{-8} to 1.2×10^{-7} Torr, as measured by an ion gauge) were generated by self-chemical ionization (self-CI). This was achieved by allowing the molecular ions and the ionic fragments of each

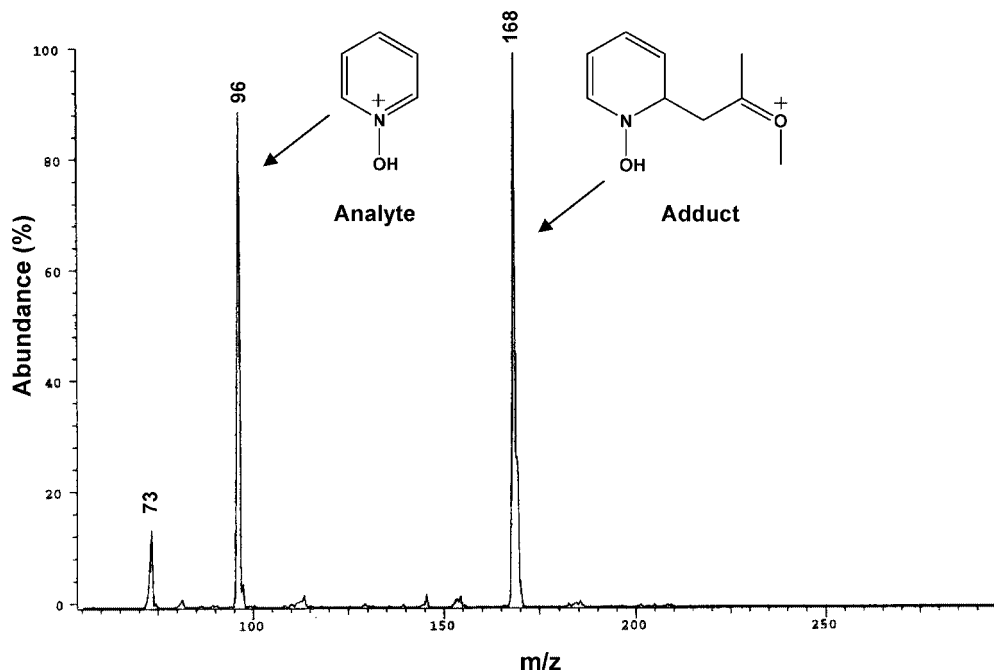


FIGURE 2. Product ion mass spectrum measured for the reaction of protonated pyridine *N*-oxide with 2-methoxypropene in the second quadrupole (Q2) of a triple quadrupole mass spectrometer. Abundant addition product of *m/z* 168 is evident. Protonated 2-methoxypropene of *m/z* 73 was also observed.

analyte, generated upon electron ionization (EI) of the analyte, to react with the neutral analyte for 0.2–6.0 s. Typical EI parameters were 0.1–1.0 s electron beam time, 25–70 eV electron energy, and 7.0 μA filament current. The protonated analyte was transferred into the other cell by grounding the conductance limit plate (80–100 μs) and was allowed to cool for 1 s via IR emission¹⁵ and collisions with argon gas pulsed into the cell (nominal pressure $\sim 1.0 \times 10^{-5}$ Torr). Prior to transfer, a negative potential of -3.5 V was applied for 12 ms to the remote trapping plate of the receiving cell to purge this cell of unwanted ions. At all other times, the three trapping plates were kept at 2 V. Nominal base pressures of the neutral reagents in this cell varied between 3.9×10^{-8} and 1.9×10^{-7} Torr, as measured by an ion gauge. The protonated analyte was isolated by using a stored-waveform inverse Fourier transform¹⁶ (SWIFT) excitation pulse to eject all unwanted ions, and allowed to react with the neutral reagent (reaction times varied from 2 to 200 s; however, up to 300 s was used to verify that no reactions took place for analytes with no aromatic *N*-oxide functionalities). Some of the reaction products were further probed by sustained off-resonance irradiation collision-activated dissociation (SORI-CAD).¹⁷ SORI-CAD experiments utilized off-resonance excitation of the isolated ion at a frequency ± 1000 Hz off the cyclotron frequency of the ion. This experiment was carried out for about 1 s in the presence of an inert gas ($\sim 10^{-5}$ Torr of argon). All the spectra were background corrected by subtracting the background spectra from the reaction spectra. Background spectra were recorded by removing the analyte ion by SWIFT ejection prior to reaction.

Triple Quadrupole Mass Spectrometer. The Finnigan TSQ 700 triple quadrupole used in this work was modified to allow for the introduction of volatile liquid reagents into the rf-only quadrupole (Q2) collision chamber. These modifications include the addition of a valve manifold to the collision gas inlet line,

and a rotary vane vacuum pump to allow freeze, pump, and thaw cycles needed to purge all dissolved gases from the liquid reagents. The analyte was introduced into the ion source via a home-built probe that was inserted into the solids probe inlet and used a Varian variable leak valve to control the analyte pressure in the source (10 mTorr nominal pressure; measured by a Granville-Phillips Convectron gauge). The protonated analyte was generated by self-chemical ionization after electron ionization (50 eV electron energy; 400 μA emission current). After the protonated analyte was mass-selected by the first quadrupole (Q1), it was allowed to undergo reactive collisions with the neutral reagent present in the second quadrupole (Q2; 5 mTorr nominal pressure; measured by a Granville-Phillips Convectron gauge) at collision energies less than 0.5 eV (set by Q2 offset voltage relative to the ion source). Reaction products were monitored by scanning the third quadrupole (Q3).

Kinetics. Kinetic measurements were carried out with only the FT-ICR mass spectrometer. Reactions studied under the conditions described above inherently follow pseudo-first-order kinetics. The pseudo-first order reaction rate constant was obtained from the negative slope of a plot of the natural logarithm of the relative abundance of the protonated analyte versus time. The second order reaction rate constant (k_{reaction}) was obtained by dividing the above pseudo-first order reaction rate constant by the absolute pressure of the neutral reagent used in the reactions. The neutral reagents' pressures were measured with ion gauges. These values were corrected for the sensitivity of the ion gauge toward the neutral reagent¹⁸ and its distance from the center of the ICR cell¹⁹ by measuring the rates of highly exothermic electron-transfer reactions between carbon disulfide radical cation and the neutral reagent. This exothermic electron transfer reaction is assumed to proceed at the collision rate. The theoretical collision rate constants ($k_{\text{collision}}$) were calculated by

(15) Dunbar, R. C. *Mass Spectrom. Rev.* **1992**, *11*, 309–339.

(16) Marshall, A. G.; Wang, T. C. L.; Chen, L.; Ricca, T. L. *ACS Symp. Ser.* **1987**, *359*, 21–33.

(17) Gauthier, J. W.; Trautman, T. R.; Jacobson, D. B. *Anal. Chim. Acta* **1991**, *246*, 211–225.

(18) Bartmess, J. E.; Georgiadis, R. M. *Vacuum* **1983**, *33*, 149–153.

(19) Leeck, D. T.; Stirk, K. M.; Zeller, L. C.; Kiminkinen, L. K. M.; Castro, L. M.; Vainiotalo, P.; Kenttämäa, H. I. *J. Am. Chem. Soc.* **1994**, *116*, 3028–3038.

using a parametrized trajectory theory.²⁰ Reaction efficiencies are given as $k_{\text{reaction}}/k_{\text{collision}}$.

Computational Studies. All calculations were performed with the Gaussian 03 suite of programs.²¹ Geometry optimizations

(20) Su, T.; Chesnavich, W. J. *J. Chem. Phys.* **1982**, *76*, 5183–5185.

(21) Frisch, M. J.; Trucks, G. W. H.; Schlegel, B.; Scuseria, G. E.; Robb, M. A.; Cheeseman, J. R.; Montgomery, J. A., Jr.; Vreven, T.; Kudin, K. N.; Burant, J. C.; Millam, J. M.; Iyengar, S. S.; Tomasi, J.; Barone, V.; Mennucci, B.; Cossi, M.; Scalmani, G.; Rega, N.; Petersson, G. A.; Nakatsuji, H.; Hada, M.; Ehara, M.; Toyota, K.; Fukuda, R.; Hasegawa, J.; Ishida, M.; Nakajima, T.; Honda, Y.; Kitao, O.; Nakai, H.; Klene, M.; Li, X.; Knox, J. E.; Hratchian, H. P.; Cross, J. B.; Adamo, C.; Jaramillo, J.; Gomperts, R.; Stratmann, R. E.; Yazyev, O.; Austin, A. J.; Cammi, R.; Pomelli, C. J.; Ochterski, W.; Ayala, P. Y.; Morokuma, K.; Voth, G. A.; Salvador, P.; Dannenberg, J. J.; Zakrzewski, V. G.; Dapprich, S.; Daniels, A. D.; Strain, M. C.; Farkas, O.; Malick, D. K.; Rabuck, A. D.; Raghavachari, K.; Foresman, J. B.; Ortiz, J. V.; Cui, Q.; Baboul, A. G.; Clifford, S.; Cioslowski, J.; Stefanov, B. B.; Liu, G.; Liashenko, A.; Piskorz, P.; Komaromi, I.; Martin, R. L.; Fox, D. J.; Keith, T.; Al-Laham, M. A.; Peng, C. Y.; Nanayakkara, A.; Challacombe, M.; Gill, P. M. W.; Johnson, B.; Chen, W.; Wong, M. W.; Gonzalez, C.; Pople, J. A. *Gaussian 03*, Revision B.03; Gaussian, Inc.: Pittsburgh, PA, 2003.

and vibrational frequency calculations were performed with use of density functional theory at the B3LYP/6-31G(d) level. Stationary points were characterized by frequency calculations to confirm a correct number of imaginary frequencies. Minimum energy structures have no imaginary frequencies. All theoretical energies are for 0 K and include zero-point vibrational energy corrections.

ACKNOWLEDGEMENT. The authors gratefully acknowledge Eli Lilly and Company for providing financial support for this work.

Supporting Information Available: Tables of Cartesian coordinates. This material is available free of charge via the Internet at <http://pubs.acs.org>.

JO800309U